



Detection of chlorinated organic pollutants with an integrated screen-printed electrochemical sensor based on a carbon nanocomposite derived from bread waste

Wenchao Duan^{a,b}, Martha Raquel Baez-Gaxiola^c, Martí Gich^{a,*}, César Fernández-Sánchez^{b,d,*}

^a Institut de Ciència de Materials de Barcelona, ICMAB (CSIC), Campus UAB, 08193 Bellaterra, Spain

^b Instituto de Microelectrónica de Barcelona, IMB-CNM (CSIC), Campus UAB, 08193 Bellaterra, Spain

^c SMARTER-Lab Nucleus for Research & Divulcation A.C., Hermosillo, Sonora, Mexico

^d CIBER de Bioingeniería, Biomateriales y Nanomedicina (CIBER-BBN), Jordi Girona 18-26, 08034 Barcelona, Spain

ARTICLE INFO

Keywords:

Sample-to-result electrochemical sensor
Ag-doped carbon nanocomposite
Bread waste
Sucralose
Trichloroacetic acid

ABSTRACT

Halogenated organic compounds are ubiquitous in water bodies due to anthropogenic activities and some of them pose a real threat to the aquatic environment and human health. That is the case of artificial sweeteners such as sucralose and haloacetic acid disinfection byproducts such as trichloroacetic acid (TCA), classified as contaminants of emerging concern. This motivates the search for rapid, cost-effective and easy-to-use analytical tools that could be deployed to facilitate the analysis of organohalide pollutants and aid in accurately monitoring water quality. This work explores the rapid detection of sucralose and TCA using a very simple miniaturized sample-to-result integrated electrochemical sensor. The device incorporates a screen-printed three-electrode electrochemical cell (SPE) where the working electrode is made of a nanocomposite of Ag nanoparticles and porous C (Ag/C). The material is prepared from bread waste, in an attempt to add value to one of the largest fractions of food leftovers and thus contribute to the sustainable circular economy. The electrochemical process behind the sensor analytical performance is initially evaluated using free Cl^- ions in solution and then, the sensor is used to analyze the mentioned target analytes. A paper disk integrated over the electrode area and loaded with the reagents required for the sample conditioning makes the analysis straightforward. The sensor thus produced can be inserted in a highly compact low-power instrument connected to a mobile phone, making an easy-to-use device suitable for on-site analytical studies.

1. Introduction

Organohalides are ubiquitous chemical species that have been recognized as pollutants or indicators of a variety of contamination events produced in the environment [1]. Among them, sucralose is a chlorinated carbohydrate that has been widely added as a sugar substitute to thousands of food products [2]. Despite its widespread use, the safety of sucralose is still controversial [3–5]. Sucralose is not easily metabolized in the human body. Indeed, it travels through the digestive system and is excreted through urine and feces, going into wastewater and eventually reaching the municipal wastewater treatment plants (WWTPs) [2]. Sucralose is very stable and not efficiently removed or transformed in WWTPs. Owing to its widespread occurrence and persistence, sucralose is cataloged as an emerging contaminant by the U.

S. Environmental Protection Agency (EPA) [6], and its monitoring and control in waters will become necessary. Another relevant organohalide pollutant is trichloroacetic acid (TCA). It is of big environmental concern due to its extensive use in agriculture and public health programs [1]. It is found in industrial wastes and as a byproduct of water chlorination [7]. TCA may enter aquatic systems via anthropogenic and natural events, including water overflow, as a degradation product of chlorinated solvents or chlorination processes including drinking water production and water disinfection of swimming pools [1]. Moreover, TCA has potential carcinogenic and mutagenic effects [8] that make its analysis and control in water mandatory.

Chromatography and mass spectrometry detection approaches currently enable the simultaneous determination of sucralose and TCA in different water matrices with adequate sensitivity and selectivity, but

* Corresponding authors.

E-mail addresses: mgich@icmab.es (M. Gich), cesar.fernandez@csic.es (C. Fernández-Sánchez).

using costly bench-top equipment, and time-consuming derivatization and extraction processes, implemented in centralized laboratories [6,9]. Up to now, few initiatives have put the focus on developing alternative analytical platforms that facilitated the rapid and reliable detection of these hazardous chemicals and could potentially be applied in-field. In this context, electrochemical detection approaches could be an excellent alternative thanks to their simplicity, instrument portability, low power requirements, and safety of operation [1,10,11]. Some nice examples can be found in the literature [1,9–14]. For instance, Nikolelis et al. reported an electrochemical sensor for the rapid screening of sucralose based on surface-stabilized bilayer lipid membranes [14]. Bashami et al. produced a highly conductive thin film of a composite integrating Ag nanoparticles (NPs) onto a commercial glassy carbon electrode (GCE) for the selective electrochemical sensing of TCA [10]. Qian, et al. prepared a voltammetric sensor for TCA using a GCE modified with Au@Ag nanorods and hemoglobin [11]. However, the major drawback of these devices is that they cannot be mass-produced because of the multi-step complex fabrication processes, including the modification of commercial bulky GCEs with specific functional materials.

Here, we describe the fabrication of a sample-to-result miniaturized electrochemical sensor for the analysis of sucralose and TCA. Ag/C screen-printed electrodes (Ag/C_SPEs) were prepared from a Ag nanoparticle-modified carbon nanocomposite whose synthesis process has been reported in our previous work [15]. This nanocomposite was produced using bread waste as the source of the carbon component, in an attempt to revalorizing one of the main food leftovers worldwide by converting it into a functional material that could also aid in the decrease of the Ag/C_SPEs fabrication costs. In order to make the sensor performance as simple and straightforward as possible, we integrated a filter paper disk loaded with chemical species over the screen-printed electrode area to enable, upon addition of a small sample volume, the automatic sample preconditioning and subsequent analyte detection. This simplified electrochemical sensor configuration combined with a compact low-power instrumentation connected to a mobile device makes it very convenient for in-field analytical studies.

2. Experimental section

2.1. Reagents and materials

All chemicals were purchased from Sigma-Aldrich and used as received, unless stated otherwise. These include potassium chloride (KCl, 99+%), sodium hydroxide (NaOH), trichloroacetic acid (99+%, Cl_3CCOOH), sucralose (98+%, chemical structure included in the Supporting Information, SI, as Figure S1), 2-butoxyethyl acetate ($\text{CH}_3\text{COOCH}_2\text{CH}_2\text{O}(\text{CH}_2)_3\text{CH}_3$), potassium nitrate (KNO_3 , 99.0%) and ferrocene-methanol ($\text{C}_{11}\text{H}_{12}\text{FeO}$, 97%). Silver nitrate (AgNO_3) was purchased from AppliChem GmbH (Germany). Ortho-phosphoric acid (85%) was used to prepare a 0.075 M phosphate buffer (PB) solution, whose pH was adjusted to 6 by adding a certain volume of a KOH solution. 0.5 mm-thick PET sheets (Autostat WP20) were purchased from MacDermid (UK). WALSRODER™ Nitrocellulose A 500 ISO 30% was purchased from Dow Wolff Cellulosics GmbH (Germany). Carbon conducting paste ref. C2030519P4 was purchased from Gwent Electronic Materials, Ltd (UK). Electrodag PF-455B photocurable dielectric and 725A silver pastes were obtained from Henkel (ES). Whatman® membrane nylon filters (pore size 0.45 μm , diam. 47 mm, WHA7404004) and self-adhesive tape (PPI Adhesive products Ltd, Lot No:375,736) were used to produce the paper disk. They were patterned using a CO_2 laser cutter (Epilog Mini 24, Epilog Laser, United States). Salt-free bread, containing less than 0.05 wt.% NaCl was bought from a local supermarket. Information about the bread composition is shown in Table S1 (SI). The bread was placed in a cool and dry place for 2 weeks, before use.

2.2. Preparation of the electrode functional material

The Ag/C nanocomposite material was prepared following the procedure reported in our previous work, with slight differences [15]. The raw materials were scaled up 15 times to obtain enough nanocomposite material for the screen printing process. In brief, 49 g of bread were immersed in 200 ml of a 0.1 M AgNO_3 water solution and left to impregnate for about 10 min. Then, the mixture was stirred slightly to get a slurry-like structure. Next, the mixture was poured into several evaporating dishes to spread it out and let it dry in a stove (60 °C) for 2 days. Thereafter, the resulting impregnated material was pyrolyzed at 1050 °C in an Ar protective atmosphere for 2 h. Finally, the carbonized material was ball-milled to obtain a powder with an average particle size of 12 μm .

2.3. Preparation of the Ag/C ink

The ink was prepared following a formulation previously reported by our group, the difference being just the Ag/C powdered material [16]. Briefly, this material was mixed with a nitrocellulose binder solution (15–20 wt.%) prepared in 2-Butoxyethyl acetate. The weight molar ratio of the Ag/C material to binder is 3:1. Afterward, the mixture was stirred thoroughly with the assistance of 2.0 mm ZrO_2 balls until the resulting paste presented a honey-like texture. The ZrO_2 balls were used to enhance the dispersion of the Ag/C powder to avoid agglomeration. Then, the ink was used to print the working electrode of the Ag/C screen-printed electrodes.

2.4. Fabrication of screen-printed electrodes

Three-electrode electrochemical cells (Figure S2, SI) were manually screen printed on PET substrates with a homemade screen-printer machine [16]. First, silver conducting tracks were printed on the PET substrate. Then, the commercial C ink was applied to print the pseudo-reference and auxiliary electrodes. In the next step, the Ag/C ink was used to print the working electrode. Finally, a dielectric layer was printed to isolate the conducting silver tracks from the environment, just leaving uncovered the contact pads and an area around the three-electrode arrangement. 12 screen-printed electrochemical cells were printed on the same PET substrate using around 0.4 g Ag/C material. 120 of these cells could be printed in one batch with around 6 g Ag/C material (Figure S2, SI). Then, they were cut into individual units with the CO_2 laser cutter (Figure S3, SI). The resulting electrochemical cell were referred as Ag/C_SPE.

2.5. Fabrication of the miniaturized analytical platform

A 1 cm-diameter paper disk (Whatman® nylon membrane filter, 0.45 μm pore size) and a vinyl plastic layer showing a holed structure (Fig. 1) were cut using the CO_2 laser cutter [16]. The paper disk was loaded with phosphate salts. For this, some 20 μl of a 0.075 M PB solution (pH 6) were drop-cast on the disk and left to dry at room temperature (Fig. 1B). Then the modified paper disk was placed covering the electrode area and was tightly fixed with a vinyl plastic layer (Fig. 1C). The resulting sample-to-result electrochemical sensor platform was named after Ag/C_SPE_paper.

The Ag/C_SPE_paper was ready to be used and just required the addition of 20 μl sample volume (Fig. 1D). This device was combined with a compact low-power minipotentiostat connected to a mobile device, for potential on-site analytical measurements (Fig. 1E).

2.6. Characterization techniques

The morphological characterization of the composite material was performed using a scanning electron microscope (SEM, Auriga from Carl Zeiss) operated at 3 – 10 kV. The Ag/C ratio was estimated by energy

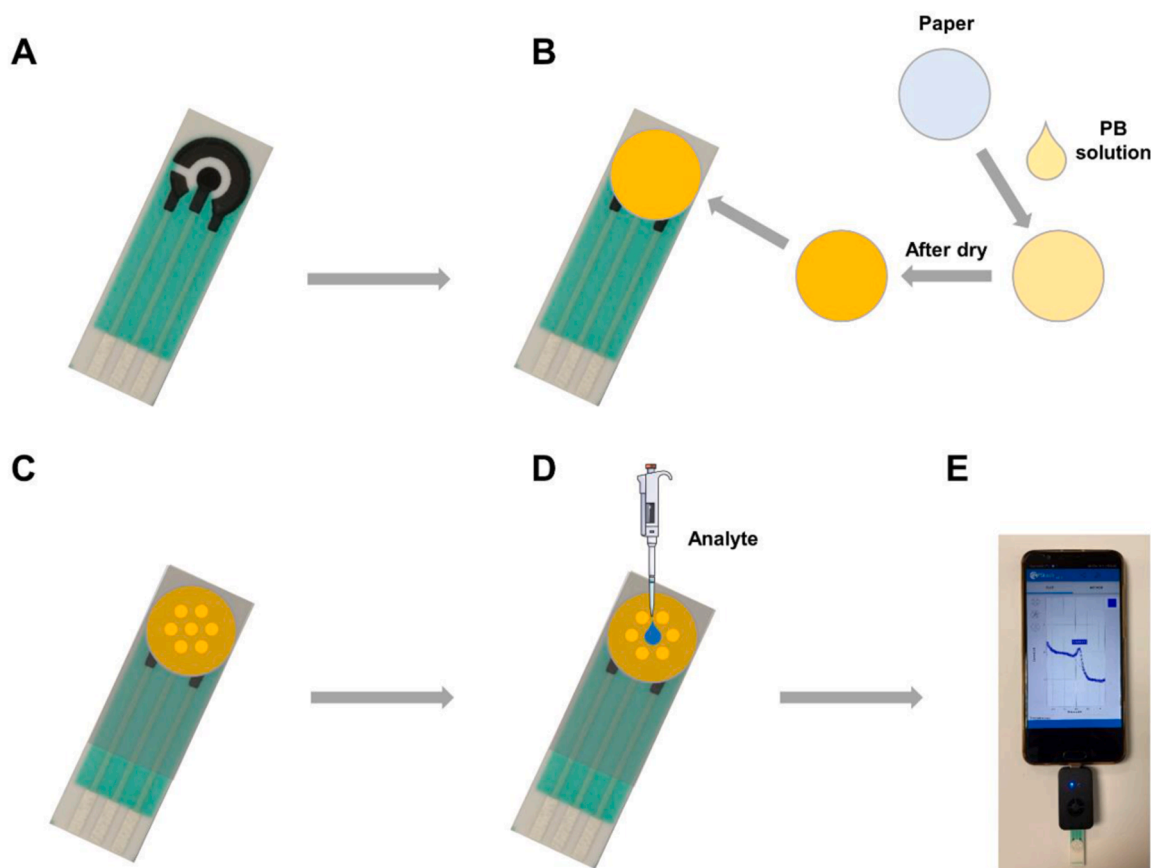


Fig. 1. Schematics of the process for integrating a filter paper disk with the Ag/C_SPE (A-C) and illustration of the simple use of the resulting Ag/C_SPE_paper (D) and its coupling to a compact low-power potentiostat connected to a mobile phone for potential deployed measurements (E).

dispersive X-ray spectroscopy (EDS).

Assessment of the electrochemical performance of the Ag/C_SPEs was initially performed using an Autolab PGSTAT30 potentiostat, controlled by NOVA v2.0 software (Metrohm Hispania, Spain). Electrochemical measurements of the compact electrochemical device in solutions of the two target analytes were conducted using the Sensit Smartphone minipotentiostat (PalmSens BV, Houten, the Netherlands), which was operated by PStouch software for Android.

All measurements were carried out by cyclic voltammetry (CV) and square wave voltammetry (SWV) techniques. In order to evaluate the electrochemical performance of the Ag/C_SPEs, CV measurements were firstly performed in a 0.1 M KNO₃ solution containing 1 mM ferrocene-methanol at 100 mV s⁻¹ scan rate. Next, CV and SWV measurements were performed for assessing the sensor analytical performance toward the detection of sucralose and TCA, respectively. The SWV parameters were 5 mV step, 25 mV amplitude and 20 Hz frequency.

3. Results and discussion

3.1. Microstructural characterization of Ag/C_SPE

Fig. 2 depicts the SEM images of the rough surface of a screen-printed working electrode made of the Ag/C nanocomposite ink. The surface morphology is similar to the surface of a commercial carbon (graphite) screen-printed electrode and the Ag/C material appears to be uniformly dispersed. The higher magnification SEM image in the secondary electron mode shown in Fig. 2C reveals the existence of small bright particles on the surface and within the bulk of the material. The bright contrasting small particles and the bulk material can be ascribed to the Ag NPs and the C component, respectively. The size distribution of the Ag NPs is between 12 nm to 18 nm, estimated with the Image J software

(Figure S4, SI) by carrying out a detailed study of different SEM images. The Ag to C ratio on the electrode surface is around 10.8 wt.% based on the EDS analysis (Figure S5, SI).

3.2. Electrochemical evaluation of the Ag/C_SPE performance

In order to evaluate the electrochemical performance of the produced Ag/C_SPEs, 20 units from the same batch were measured in a 0.1 M KNO₃ solution containing 1 mM ferrocene-methanol reversible electroactive species at a potential scan rate of 100 mVs⁻¹. Fifteen of them provided comparable signals, showing a peak-to-peak separation (ΔE_p) and an anodic to cathodic peak current ratio of 187 ± 7 mV and 0.94 ± 0.02 , respectively (Table S2, SI). Thus, the fabrication yield was estimated to be 75%. Figure S6 (SI) shows three examples of the CVs recorded with the Ag/C_SPEs. Even though the fabrication yield was not high, this could be increased by optimizing different aspects of the material synthesis, such as the effective mixing of bread waste and Ag precursor or the use of an automatic screen-printing machine. Nevertheless, the protocol described above was implemented in the lab to assess the electrochemical performance of the Ag/C_SPEs and select those ones that were further used for measuring halide compounds, as described below.

The CV of the Ag/C_SPE was recorded in 0.075 M PB background solution (pH = 6) to show the electrochemical redox processes that the Ag NPs underwent (Fig. 3). The well-defined anodic peak at +0.27 V (vs. C pseudo-ref. electrode) could be ascribed to the oxidation of Ag and the formation of Ag₂O [17–19]. Two other anodic processes are visible at around +0.15 V and +0.45 V that could be ascribed to the formation of Ag(OH) and AgO, respectively. The cathodic peak centered at around -0.15 V (vs. C pseudo-ref. electrode) could be related to the reduction of the Ag oxides and the formation of Ag⁰ species on the electrode surface

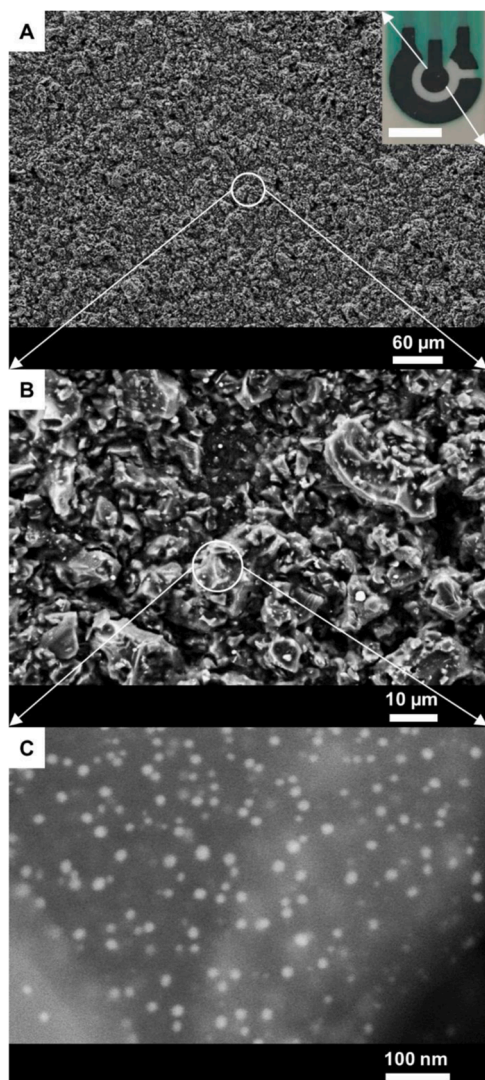


Fig. 2. SEM images of the surface of a Ag/C composite screen-printed electrode at different magnifications. Inset in (A) is a photograph of the SPE three-electrode cell. The scale bar is 0.5 cm.

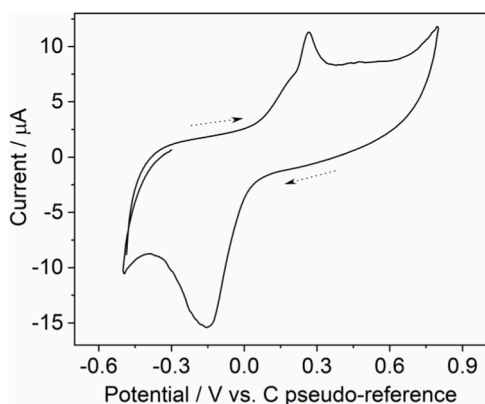


Fig. 3. Cyclic voltammogram in PB solution (pH = 6.0) using a Ag/C screen-printed composite electrode at a scan rate of 100 mVs⁻¹. The arrows indicate the potential scan direction.

[17–19]. These processes were similar to those observed in the characterization of the Ag/C material using carbon paste electrodes [15]. Although the peak definition could be further improved by finely tuning the ink composition and screen-printing fabrication process, the electrochemical performance of commercial SPEs is often not as good as that of the bulky electrode counterparts, such as glassy carbon or pyrolytic graphite electrodes. This is likely due to the ink composition showing a low mass percentage of the conductive material (75 wt.% for the Ag/C conductive material in this work).

Cl⁻ was initially used as a standard analyte to explore the performance of the Ag/C SPEs for detecting chlorinated species. Fig. 4 shows the CV signals recorded in Cl⁻ solutions in a concentration range from 50 μM to 2723 μM. There is an apparent increase in the peak current recorded at around +0.19 V (vs. C pseudo-ref. electrode) with the increase of Cl⁻ concentration in solution. This peak was recorded at a lower overpotential than that related to the oxidation of Ag when no Cl⁻ ions are present in solution (Fig. 3). It could be ascribed to the oxidation of Ag⁺ favored by the production of a AgCl precipitate on the AgNP surface. Also, the peak potential shifted towards more negative values with the increase of Cl⁻ concentration as can be expected from the Nernst equation [20,21]. A calibration curve was constructed and the corresponding analytical parameters were summarized in Table 1. Two linear ranges were observed, showing a behavior similar to that of the Ag/C material tested using carbon paste electrodes and a standard electrochemical cell [15]. A limit of detection in the low μM range was estimated. Electrochemical measurements showed a good reproducibility reflected in the low coefficients variation that were below 5%, for all the concentrations measured. Then, studies were conducted to

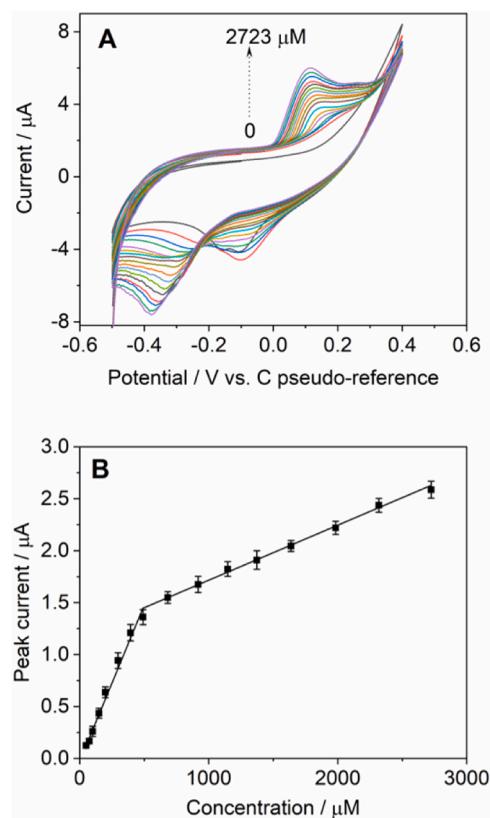


Fig. 4. (A) Cyclic voltammograms recorded with Ag/C SPE in PB solutions containing from 50 μM to 2723 μM Cl⁻ (the signals from bottom to top correspond to: 0, 50, 74, 100, 149, 199, 297, 395, 491, 682, 917, 1147, 1373, 1639, 1983, 2318 and 2723 μM), scan rate 100 mVs⁻¹. (B) Calibration curve of the Ag/C SPE for measurement of Cl⁻. Each point represents the mean value of three measurements carried out with three electrochemical sensors from the same batch, the error bars being the corresponding standard deviation.

Table 1
Analytical parameters obtained from the calibration curves for Cl^- , sucralose and TCA analysis.

sensor	analyte	method	slope ($\text{nA } \mu\text{M}^{-1}$)	intercept (μA)	R[2] ($n = 3$)	LOD (μM)	Linear range (μM)
Ag/C_SPE	Cl^-	CV	3.0 ± 0.1	0.030 ± 0.006	0.991	15.2	50–491
			0.50 ± 0.02	1.20 ± 0.02	0.994	-	491–2723
	sucralose	CV	0.20 ± 0.01	1.80 ± 0.01	0.993	145	200–2920
Ag/C_SPE_paper	TCA	SWV	0.030 ± 0.001	2.20 ± 0.01	0.991	-	3850–16,690
			0.300 ± 0.003	0.70 ± 0.01	0.999	19.8	100–5508
	sucralose	CV	0.200 ± 0.004	0.20 ± 0.01	0.994	240	400–2920
			0.070 ± 0.001	0.70 ± 0.02	0.998	-	3850–13,070
TCA	SWV	0.200 ± 0.002	0.300 ± 0.001	0.999	23.8	100–4295	

*Limit of detection (LOD) is calculated using the 3σ IUPAC criterion.

monitor sucralose and trichloroacetic acid in waters as representative examples of organochloride water contaminants.

It should be pointed out that these studies and the ones described below were carried out in the same background electrolyte, that is a 0.075 M PB solution pH 6. Solutions at different pHs were previously tested [15] but the electrochemical signals recorded at pH 6 showed a better discrimination between the anodic peak related to the formation of the AgCl precipitate and the ones ascribed to the production of different silver oxide species (Fig. 3).

3.3. Electrochemical detection of sucralose and TCA using the Ag/C_SPE

Fig. 5 shows the cyclic voltammograms recorded with Ag/C_SPE in PB solutions containing increasing concentrations of sucralose. A peak at

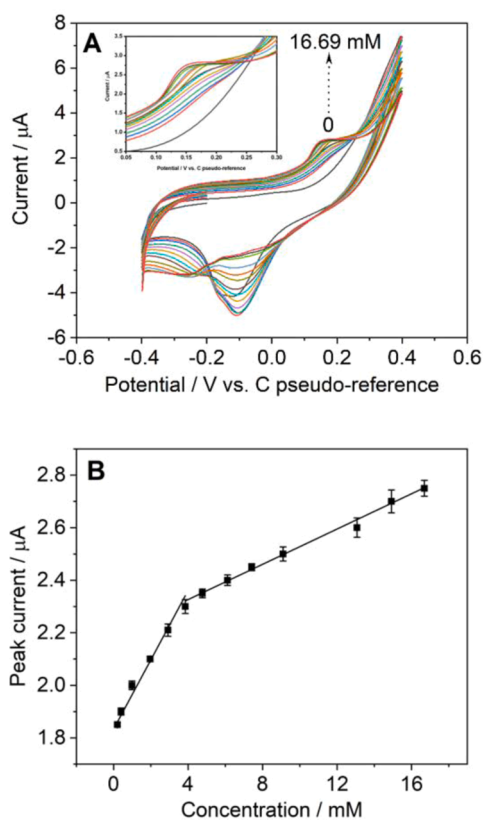


Fig. 5. (A) Cyclic voltammograms recorded with Ag/C_SPE in PB solutions containing from 0 to 16.69 mM sucralose (the signals from bottom to top correspond to: 0, 0.2, 0.4, 0.99, 1.97, 2.92, 3.85, 4.77, 6.12, 7.42, 9.11, 13.07, 14.92 and 16.69 mM), scan rate 100 mVs^{-1} . (B) Zoomed in image of the cyclic voltammograms shown in (A). (C) Calibration curve of the Ag/C_SPE for sucralose. Each point represents the mean value of three measurements carried out with three electrochemical sensors from the same batch, the error bars being the corresponding standard deviation.

around $+0.18 \text{ V}$ was recorded, at a value very close to that observed in the measurements of free Cl^- in solution. This peak may also be related to the oxidation of Ag favored by the formation of a AgCl precipitate with Cl^- ions present in solution. The formation of free Cl^- ions may be produced in solution upon the cleavage of the sucralose C—Cl bonds. This process appeared to also be catalyzed by the AgNPs, as explained in detail in a previous publication of our group [15]. Briefly, a two step process may take place. Initially, the target analyte undergoes a dehalogenation step via the formation of an attenuated radical intermediate between the halogenated species and Ag, which rapidly induces the break of the C—Cl bond and the release of Cl^- ions. Then, free Cl^- ions adsorb on the AgNP surface, reacting with Ag to form AgCl.

Peak currents increased upon increasing the sucralose concentration in solution. The corresponding calibration curve was constructed, and the extracted analytical parameters are gathered in Table 1. The calibration curve also shows two linear ranges and a limit of detection of $145 \mu\text{M}$ was estimated.

The detection of TCA was firstly attempted by CV. The sensor showed a limited sensitivity and a limit of detection in the mM range (data not shown). As in a previous report by B. Liu et al. [7], square wave voltammetric (SWV) measurements were attempted aiming at improving the sensor analytical performance. Figure S7 (SI) shows the SWV signal recorded with the Ag/C_SPE in 0.075 M PB solution (pH = 6.0). An anodic peak at around $+0.28 \text{ V}$ was observed, which can be ascribed to the oxidation of Ag NPs. This result is in accordance with the CV measurement shown in Fig. 3.

Then, square wave voltammograms were recorded in PB solutions containing TCA. First, three parameters influencing the SWV response were optimized. These were the applied conditioning potential and conditioning potential time together with the initial scan potential (Figure S8, SI). An anodic peak at around $+0.12 \text{ V}$ (vs. C pseudo-reference) was ascribed to the electrocatalytic reaction of TCA with the electrochemical sensor, while the peak at around $+0.28 \text{ V}$ corresponds to the direct oxidation of Ag NPs on the electrode surface. However, the peak related to the detection of the TCA target species was not observed when the applied conditioning potential was below 0 V (Figure S8A). As this potential value increased steadily from $+0.15 \text{ V}$ to $+0.7 \text{ V}$, the recorded peak at $+0.12 \text{ V}$ appeared and its peak current increased, becoming predominant at conditioning potentials values $\geq +0.3 \text{ V}$. A clear explanation for this behavior cannot be given. However, we hypothesized that the application of these conditioning potential values might induce an activation of the Ag NPs. That is, Ag NPs were oxidized to a certain extent, generating Ag^+ species that were required for the effective interaction of the TCA target analyte with the Cl^- residues. From the voltammograms shown in Figure S8A, a $+0.5 \text{ V}$ potential was selected for further experiments. Regarding the influence of the initial scan potential, Figure S8B shows that this potential should be lower than -0.05 V for recording the TCA peak. Two separated small peaks appear when the starting potential was set to -0.1 V . By decreasing this value to -0.3 V or -0.5 V , the TCA peak increased and was better defined. Thus, the selected potential scan range was between -0.5 V and $+0.6 \text{ V}$. Next, the conditioning potential time was optimized in the measurements presented in Figure S8C. As the time increased

from 15 s to 30 s, 60 s and 120 s, the peak intensity for measuring TCA slightly increased when the applied time was 15 and 30 s, and then it decreased, the effect being more dramatic for longer conditioning times. This behavior might be related to activation of the AgNPs, as explained above, at short activation times and the excessive oxidation and in turn degradation of the AgNPs upon application of the conditioning potential for times longer than 60 s. Thus, 30 s was used for further measurements.

Sensor SWV responses were recorded in solutions containing TCA. Figure S7B (SI) shows SWVs for three different TCA concentrations in the potential range from -0.5 V to $+0.25$ V. The peak ascribed to the detection of TCA increased with the TCA solution concentration, as expected. Fig. 6A shows the sensor responses for the whole TCA concentration range assayed. The calibration curve was then plotted (Fig. 6B) and the corresponding analytical parameters are included in Table 1. A linear response in the concentration range of 100 - 5508 μM TCA was obtained, with a sensitivity of 0.3 ± 0.003 $\text{nA } \mu\text{M}^{-1}$. The LOD was 19.8 μM , estimated using the 3σ IUPAC criterion [22].

3.4. Electrochemical detection of sucralose and TCA using the complete analytical sensor platform

As previously described in the Experimental section, in order to make the Ag/C,SPE sensor of potential use for on-site analysis, a paper disk loaded with the reagents required for sample conditioning, was implemented over the sensor area (Ag/C,SPE_paper). The paper disk allows for the sample filtering and pH and ionic conductivity adjustment in an

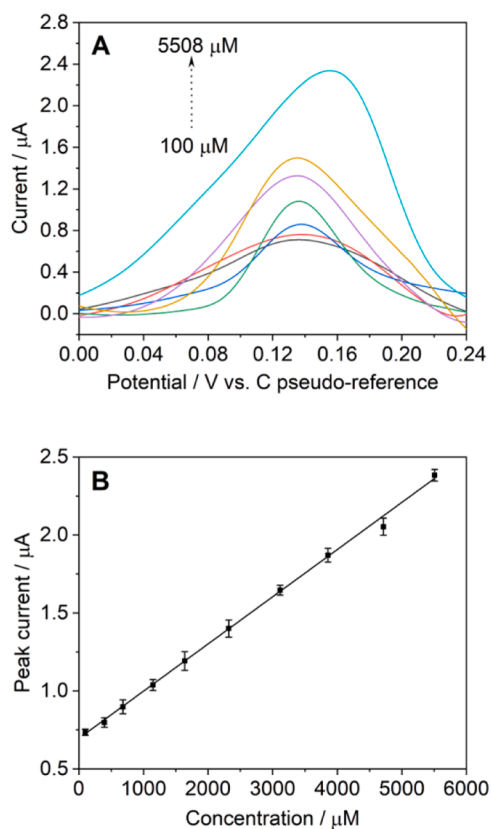


Fig. 6. (A) Square-wave voltammograms of some representative concentrations of TCA recorded with Ag/C,SPE electrode (the signals from bottom to top correspond to: 100, 395, 682, 1639, 2318, 3114, and 5508 μM); (B) Calibration curve for the measurement of trichloroacetic acid using SWV method. Each point represents the mean value of three measurements carried out with three electrochemical sensors from the same batch, the error bars being the corresponding standard deviation. The SWV parameters were 5 mV step, 25 mV amplitude and 20 Hz frequency. A baseline correction was carried out to better visualize the peak signals.

automatic fashion. Thus, the addition of 20 μl of sample was just required for carrying out one measurement, producing a sample-to-result sensor device. The developed sensor was combined with a miniaturized potentiostat connected to a smartphone in order to get a highly compact analytical platform for deployed in-field analysis (Fig. 1 and Fig. 7). A similar electrochemical sensor architecture was previously reported by us for measuring chemical oxygen demand [16].

CV measurements were carried out using water solutions containing different concentrations of sucralose with the Ag/C,SPE paper platform. The addition of 20 μl of a solution over the paper disk area produces the dissolution of the phosphate salts loaded in the paper that allowed the adjustment of the phosphate concentration in solution to 0.075 M and of the pH to 6, thus obtaining the same experimental conditions to those used in the previous studies using the Ag/C,SPE. Fig. 8 shows a zoom image of the recorded peak. It can be seen that the current of the anodic peak ascribed to the sucralose detection increased with the sucralose concentration. Accordingly, the calibration curve was obtained and the corresponding analytical parameters are summarized in Table 1. The calibration curve also shows two linear ranges. The range at low concentrations between 0.4 mM and 2.92 mM, shows a higher slope than the second range between 3.85 mM to 13.07 mM. These values are in the same range as those obtained with the Ag/C,SPE device.

Finally, the same platform was used to measure TCA by SWV. Fig. 9A and 9B show the SWV sensor responses at different concentrations of TCA and the corresponding calibration. The analytical parameters were shown in Table 1 and, again, a similar behavior to that observed with the Ag/C,SPE sensor was demonstrated.

Previous reports describing similar sensor approaches were sought for comparative purposes. To the best of our knowledge, the detection of sucralose using an electrochemical sensor platform was just reported in one paper by Nikolelis et al.. This sensor approach incorporated a surface-stabilized bilayer lipid membrane. A change in the ionic conductivity of the membrane was produced upon adsorption of the target analyte that transduced into a faradaic current using a two-electrode configuration, whose value was directly proportional to the analyte concentration in solution [14]. This work just reports a proof-of-concept of a sensor transduction mechanism using lipid membrane receptors, which was not explored any further. Moreover, the sensor lifetime was short and proved to be difficult to implement in decentralized analytical studies.

Electrochemical sensor approaches for TCA detection were previously reported and are summarized in Table S3 (SI). Some of these outperform the sensor described in our work in terms of linear range and limit of detection. However, most of them are based on complex sensor architectures, thus making the manufacturing process unsuitable for mass production purposes. In addition, the use of conventional electrochemical cells comprising commercial working electrodes such as glassy carbon, restricts their use to laboratory bench-top analytical studies.

4. Conclusion

A sample-to-result miniaturized Ag/C,SPEs paper electrochemical sensor was successfully fabricated and showed the potential to be applied to detect sucralose and TCA in water samples. 40 g bread waste could be used for producing a functional carbon material composite doped with Ag NPs that could be processed as an ink to batch fabricate around 200 electrochemical sensors by screen-printing technology. The analysis performance of the Ag/C,SPEs electrochemical sensor toward the detection of chlorinated compounds was demonstrated by firstly detecting free Cl^- in solution and then detecting sucralose and TCA representative chlorinated organic pollutants at sub-mM concentrations by cyclic and square-wave voltammetric techniques. By integrating a modified paper disk with the Ag/C,SPEs, a compact analytical platform was eventually constructed that successfully performed in the analysis of the selected target species. Although the presented sensor platform

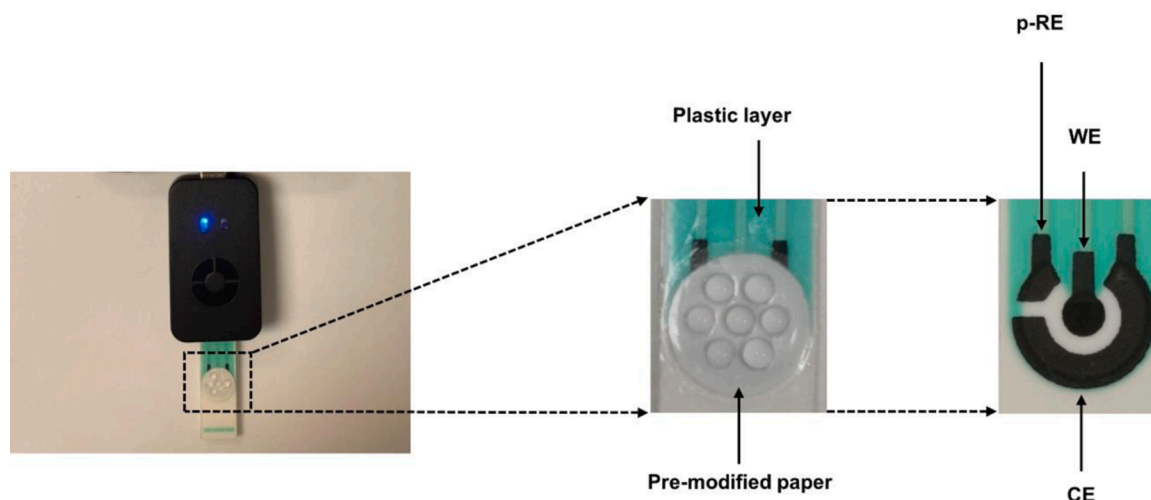


Fig. 7. Photograph of the Ag/C_{SPE} sensor with and without the implemented paper disk and the connection to a compact low-power minipotentiostat for in-field measurements.

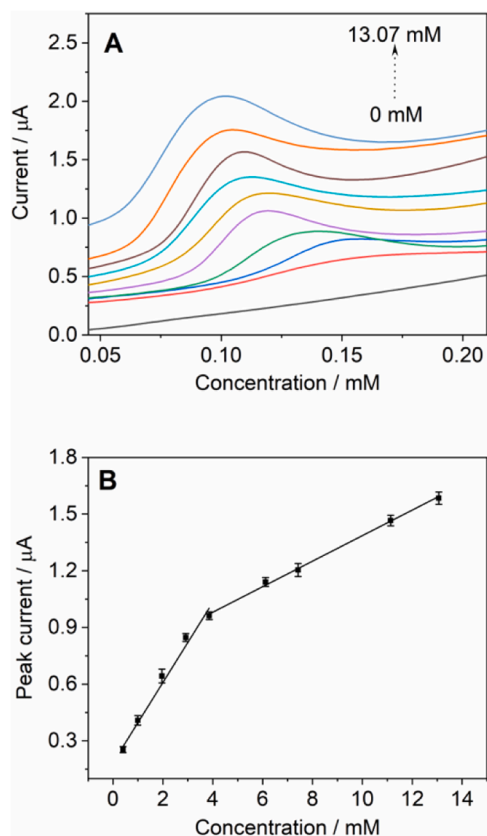


Fig. 8. (A) Cyclic voltammograms recorded with Ag/C_{SPE} paper sensor connected to the smartphone-based minipotentiostat at different concentrations of sucralose (the signals from bottom to top correspond to: 0, 0.4, 0.99, 1.97, 2.92, 3.85, 6.12, 7.42, 11.13 and 13.07 mM), scan rate 100 mV s⁻¹. (B) Corresponding calibration curve. Each point represents the mean value of three measurements carried out with three electrochemical sensors from the same batch, the error bars being the corresponding standard deviation.

could be further improved to enhance the overall analytical performance, it shows how a simple and cost-effective batch manufacturing process could mass produce an analytical tool for detecting chlorinated compounds to be readily applied in decentralized analytical studies.

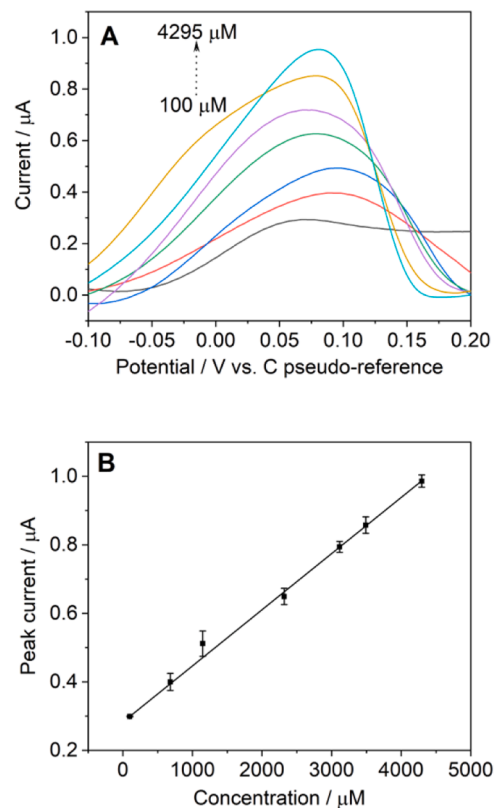


Fig. 9. (A) SWVs recorded with Ag/C_{SPE} paper sensor connected to the smartphone-based minipotentiostat at different concentrations of TCA (the signals from bottom to top correspond to: 100, 682, 1147, 2318, 3114, 3491 and 4295 μM), (B) Calibration curve for the measurement of trichloroacetic acid. Each point represents the mean value of three measurements carried out with three electrochemical sensors from the same batch, the error bars being the corresponding standard deviation. The SWV parameters were 5 mV step, 25 mV amplitude and 20 Hz frequency. A baseline correction was carried out to better visualize the peak signals.

CRediT authorship contribution statement

Wenchao Duan: Methodology, Validation, Formal analysis, Investigation, Writing – original draft, Writing – review & editing. Martha

Raquel Baez-Gaxiola: Methodology, Formal analysis, Investigation.
Martí Gich: Conceptualization, Methodology, Writing – original draft, Writing – review & editing, Supervision, Funding acquisition.
César Fernández-Sánchez: Conceptualization, Methodology, Writing – original draft, Writing – review & editing, Supervision, Funding acquisition.

Declaration of Competing Interest

The authors declare that they have no known competing financial interests or personal relationships that could have appeared to influence the work reported in this paper.

Data Availability

The raw/processed data required to reproduce these findings cannot be shared at this time due to technical or time limitations

Acknowledgments

The Chinese Scholarship Council fellowship (201806220063) to W. C. Duan is acknowledged. WD is enrolled in the Materials Science Ph.D. Program of the UAB (Universitat Autònoma de Barcelona). The X-ray diffraction and thermal analysis laboratories of the ICMAB scientific services contributed to this work and are acknowledged. This work used the Spanish ICTS Network MICRONANOFABS which was partly supported by the Spanish Ministry of Science and Innovation. This work was also partially funded by the Spanish Ministry of Science and Innovation through the Severo Ochoa program for Centers of Excellence in R&D (CEX2019-000917-S).

Supplementary materials

Supplementary material associated with this article can be found, in the online version, at doi:[10.1016/j.electacta.2022.141459](https://doi.org/10.1016/j.electacta.2022.141459).

References

- [1] M. Kurd, A. Salimi, R. Hallaj, Highly sensitive amperometric sensor for micromolar detection of trichloroacetic acid based on multiwalled carbon nanotubes and Fe (II)-phtalocyanine modified glassy carbon electrode, *Mater. Sci. Eng.: C* 33 (3) (2013 Apr 1) 1720–1726.
- [2] Y. Xu, Y. Wu, W. Zhang, X. Fan, Y. Wang, H. Zhang, Performance of artificial sweetener sucralose mineralization via UV/O₃ process: kinetics, toxicity and intermediates, *Chem. Eng. J.* 353 (2018 Dec 1) 626–634.
- [3] B.A. Magnuson, A. Roberts, E.R. Nestmann, Critical review of the current literature on the safety of sucralose, *Food Chem. Toxicol.* 106 (2017 Aug 1) 324–355.
- [4] J.H. Park, G.B. Carvalho, K.R. Murphy, M.R. Ehrlich, W.J. William, Sucralose suppresses food intake, *Cell Metab.* 25 (3) (2017 Mar 7) 484–485.
- [5] Q.P. Wang, S.J. Simpson, H. Herzog, G.G. Neely, Chronic sucralose or l-glucose ingestion does not suppress food intake, *Cell Metab.* 26 (2) (2017 Aug 1) 279–280.
- [6] S.D. Richardson, S.Y. Kimura, Water analysis: emerging contaminants and current issues, *Anal. Chem.* 92 (1) (2019 Dec 11) 473–505.
- [7] B. Liu, X. Hu, Y. Deng, S. Yang, C. Sun, Selective determination of trichloroacetic acid using silver nanoparticle coated multi-walled carbon nanotubes, *Electrochem. Commun.* 12 (10) (2010 Oct 1) 1395–1397.
- [8] J.M. Wright, J. Schwartz, D.W. Dockery, The effect of disinfection by-products and mutagenic activity on birth weight and gestational duration, *Environ. Health Perspect.* 112 (8) (2004 Jun) 920–925.
- [9] B. Liu, Y. Deng, X. Hu, Z. Gao, C. Sun, Electrochemical sensing of trichloroacetic acid based on silver nanoparticles doped chitosan hydrogel film prepared with controllable electrodeposition, *Electrochim. Acta* 76 (2012 Aug 1) 410–415.
- [10] R.M. Bashami, M.T. Soomro, A.N. Khan, E.S. Aazam, I.M. Ismail, M.S. El-Shahawi, A highly conductive thin film composite based on silver nanoparticles and malic acid for selective electrochemical sensing of trichloroacetic acid, *Anal. Chim. Acta* 1036 (2018 Dec 7) 33–48.
- [11] D. Qian, W. Li, F. Chen, Y. Huang, N. Bao, H. Gu, C. Yu, Voltammetric sensor for trichloroacetic acid using a glassy carbon electrode modified with Au@ Ag nanorods and hemoglobin, *Microchim. Acta* 184 (7) (2017 Jul) 1977–1985.
- [12] S. Palanisamy, C. Karupiah, S.M. Chen, P. Periakaruppan, A highly sensitive and selective enzymatic biosensor based on direct electrochemistry of hemoglobin at zinc oxide nanoparticles modified activated screen printed carbon electrode, *Electroanalysis* 26 (9) (2014 Sep) 1984–1993.
- [13] H. Dai, H. Xu, X. Wu, Y. Lin, M. Wei, G. Chen, Electrochemical behavior of thionine at titanate nanotubes-based modified electrode: a sensing platform for the detection of trichloroacetic acid, *Talanta* 81 (4–5) (2010 Jun 15) 1461–1466.
- [14] D.P. Nikolelis, S. Pantoulis, A minisensor for the rapid screening of sucralose based on surface-stabilized bilayer lipid membranes, *Biosens. Bioelectron.* 15 (9–10) (2000 Nov 1) 439–444.
- [15] W. Duan, C. Fernández-Sánchez, M. Gich, Upcycling bread waste into a Ag-doped carbon material applied to the detection of halogenated compounds in waters, *ACS Appl. Mater. Interfaces* 14 (35) (2022 Aug 23) 40182–40190.
- [16] W. Duan, F.J. del Campo, M. Gich, C. Fernández-Sánchez, In-field one-step measurement of dissolved chemical oxygen demand with an integrated screen-printed electrochemical sensor, *Sens. Actuators B* (2022 Jul 3), 132304.
- [17] J.M. Droog, P.T. Alderliesten, G.A. Bootsma, Initial stages of anodic oxidation of silver in sodium hydroxide solution studied by potential sweep voltammetry and ellipsometry, *J. Electroanal. Chem. Interfacial. Electrochem.* 99 (2) (1979 May 25) 173–186.
- [18] A. Bayesov, E. Tuleshova, A. Tukibayeva, G. Aibolova, F. Baineys, Electrochemical behavior of silver electrode in sulphuric acidic solution during anodic polarization, *Orient. J. Chem.* 31 (4) (2015) 1867.
- [19] P. Stonehart, F.P. Portante, Potentiodynamic examination of surface processes and kinetics for the Ag₂O/AgO/OH– system, *Electrochim. Acta* 13 (8) (1968 Aug 1) 1805–1814.
- [20] B. Patella, G. Aiello, G. Drago, C. Torino, A. Vilasi, A. O’Riordan, R. Inguanta, Electrochemical detection of chloride ions using Ag-based electrodes obtained from compact disc, *Anal. Chim. Acta* 1190 (2022 Jan 15), 339215.
- [21] F. Pargar, H. Kolev, D.A. Koleva, K van Breugel, Microstructure, surface chemistry and electrochemical response of Ag| AgCl sensors in alkaline media, *J. Mater. Sci.* 53 (10) (2018 May) 7527–7550.
- [22] L.A. Currie, Nomenclature in evaluation of analytical methods including detection and quantification capabilities (IUPAC Recommendations 1995), *Pure Appl. Chem.* 67 (10) (1995 Jan 1) 1699–1723.